Article

Numerical Simulation of Carbon Tetrachloride Pollution-Traceability in Groundwater System of an Industrial City

Benli Guo [1,2,3,4], **Peng Yang** [1,2,3,4], **Yan Zhou** [5,*], **Hongjian Ai** [1,2,3,4], **Xiaodong Li** [1,2,3,4], **Rifei Kang** [1,2,3,4] **and Youcheng Lv** [1,2,3,4]

1   No.8 Institute of Geology and Mineral Resources Exploration of Shandong Province, Rizhao 276826, China
2   Key Laboratory of Nonferrous Metal Ore Exploration and Resource Evaluation of Shandong Provincial Bureau of Geology and Mineral Resources, Rizhao 276826, China
3   Rizhao Big Data Research Institute of Geology and Geographic Information, Rizhao 276826, China
4   Rizhao Key Laboratory of Land Quality Evaluation and Pollution Remediation, Rizhao 276826, China
5   School of Water Resources and Environment, China University of Geosciences (Beijing), Beijing 100083, China
*   Correspondence: yzhou@cugb.edu.cn

Abstract: Carbon Tetrachloride (CCL4) is a colorless, volatile, and toxic liquid. Once it pollutes groundwater, it will not only destroy the ecological environment but also negatively affect the functioning of the human liver. An industrial city in eastern China has been contaminated with carbon tetrachloride (CCL4). Due to the complex hydrogeological conditions, it is difficult to determine the pollution source by a single hydrochemical analysis. In order to solve the traceability problem, in this work we established a traceability system by combining hydrochemical analysis, backward tracing, and forward transport, and analyzed the pollution distribution, pollution-source location and pollution-transport characteristic in groundwater, which provided technical support for CCL4-pollution control of groundwater in this area. (1) Groundwater samples were analyzed using the gas chromatography/mass spectrometry method. Through the pollution concentration-field, we identified the location of the pollution center and the concentration value in the northeast and southwest, screening out the monitoring wells exceeding the criteria: HF#1, DJ#19, DJ#7, SS#4, ZF#2, and DY#3. (2) Backward tracing over the past 30 years and 50 years was conducted through MODPATH. Potential polluting factories were identified by comparing the capture area with the historical distribution of factories. (3) Forward solute-transport was performed at the location of these potentially polluted factories. The distribution characteristics of pollutants in limestone layers and the Quaternary layer were analyzed using a simulated concentration-field for August 2012 and October 2016. (4) Comparing the simulated concentration with the observed concentration, the source of CCL4 pollution was inferred to be the textile mill in the 1990s, the steelworks in the 1970s, and the machine-tool plant in the 1970s and 1990s. Based on the concentration–duration curve at the pollution source, the transport characteristics and the transport speed of the pollutants in the study area were analyzed. This work not only successfully found the location of CCL4-pollution sources, but also helped the local government to analyze the year of pollutant release and recognize the transport pattern of CCL4 in aquifers.

Keywords: traceability; numerical simulation; MODPATH; carbon tetrachloride

1. Introduction

With the development of the social economy, the impact of human activities on groundwater pollution is more and more obvious [1]. Groundwater pollution has the characteristics of invisibility, complexity and delay in discovery. Pollutants can usually be adsorbed in the soil for a long time, and will continue to diffuse and infiltrate into

the groundwater to form pollution, threatening human health [2]. Among them, Carbon Tetrachloride pollution is particularly concerning [3].

Carbon Tetrachloride (CCL4) is a toxic liquid, which is colorless, volatile, slightly soluble in water, and easily soluble in most organic solvents [4]. It has been widely used in industry, for decades as an industrial degreasing-agent, pesticide, flame retardant, and for dry cleaning [5]. Studies have shown that prolonged exposure to the CCL4 compound on the human body can cause a number of complications, negatively affecting the functioning of the liver, and the occurrence of malignant tumors, which take several months to develop [6]. Since 1960, there have been studies on carbon tetrachloride pollution in the United States, Finland and China. Research shows that CCL4 pollution is generally widespread, the pollution source unclear, and it is difficult to treat [7–9].

The first step in groundwater CCL4-pollution control is to trace the source of pollutants, which is to find out the location of pollution sources and the history of pollutant migration and transformation, through limited observational-data [10,11]. Groundwater-tracing techniques mainly include the geochemical-footprint method and numerical simulation. Among these, the geochemical-footprint method uses isotopic fingerprints or geostatistical analysis to obtain pollution-source information [12]. However, using the geochemical-footprint method alone cannot completely trace the location of pollution sources and obtain the transport path of pollutants over time, and, especially when the source of pollution is not specified, this method is difficult to apply [13].

With the development of computing technology, numerical simulation has gradually become an important tool for hydrological study. The solute-transport model is an effective method to trace the source of pollution caused by point sources [14]. For example, the MODPATH module can solve the pollution-source identification problems using inverse-solution approaches [15]. In the Lombardy region, one of the most industrialized areas in Italy, MODPATH was used to find multiple-point sources of groundwater pollution [16]. In central-eastern Tuscany, the source of Boron pollution in the shallow groundwater was traced [17]. The accuracy of MODPATH tracing is closely related to the location of contamination. If the polluted monitoring-point is not a typical site along the pollution-transport route, it will lead to the deviation of the source location. In addition, too many pollution monitoring points will also lead to the problem of multiple pollution sources, making it impossible to effectively search for pollution sources.

MT3D are well-known three-dimensional groundwater flow and pollution-transport modules. It has many applications in pollutant forward-transport and pollution plume-prediction. Zhang et al. used the MT3DMS module in GMS numerical-simulation software to establish the migration and transformation model of typical chlorinated hydrocarbons [18]. M Wen et al. established a solute-transport model based on the sampled data to predict CCL4 pollution in the study area over the next 15 years [19]. Therefore, MT3D is suitable for contamination-transport modeling of the watershed under transient conditions. MODPATH can achieve the target of source tracing, but it has uncertainty and cannot analyze the transport of pollutants [20,21]. Therefore, the combination of MODPATH and MT3D is an effective traceability method, and can greatly reduce the uncertainty of the simulation.

In an industrial city in China, CCL4 pollution was found in samples of groundwater. In the study area, single hydrochemical-analysis has been unable to obtain the location of the source of pollution. Using the MODPATH tool to carry out the backward-tracing work produces great uncertainty. Therefore, in this work, we adopted the method of combining hydrochemical analysis, backward tracing, and forward simulation, to trace the source of pollutants over the past 30 and 50 years. Based on the historical factory-distribution, the location of the pollution source was delineated, and the transport characteristic of pollutants was analyzed. This work provides scientific evidence for pollutant treatment in the study area.

2. Material and Methods

2.1. Study Area

The study area is located in the economically developed area of eastern China, a political, economic, and cultural center, with a catchment area of 400 km^2. The elevation of this area is between 24 and 387 m. The climate type in the area is a continental-monsoon climate, with an average annual temperature of 13.7 °C and an average annual rainfall of 651 mm. Rainfall is concentrated from June to August, accounting for 65% of annual rainfall. The average annual evaporation is 1759 mm, and the maximum humidity is in July and August, with relative humidity 75~80%.

The flow direction of groundwater in the study area is generally from south to north, as shown in Figure 1. Affected by the high-intensity pumping of the water-supply source, there is a groundwater-drawdown cone in the north. In the south part, there are low hills with outcropping limestone. Because the overlying Quaternary sediments are very thin, it is a single-karst aquifer. The north part is a piedmont inclined-plain with magmatic intrusions located in the west. The Quaternary sediments gradually become thicker, with a thickness between 20 and 100 m, so there is an exchange between the lower karst-aquifer and upper Quaternary-aquifer. At the northwestern boundary, there develops a main river about 4 m deep and 100 m wide. Tributaries 1 and 2 originate from the mountainous area in the south, and both flow into the main river. Near the northern border, there are spring groups exposed in the northern part of the study area, and the flow rate is 3000–4000 m^3/d.
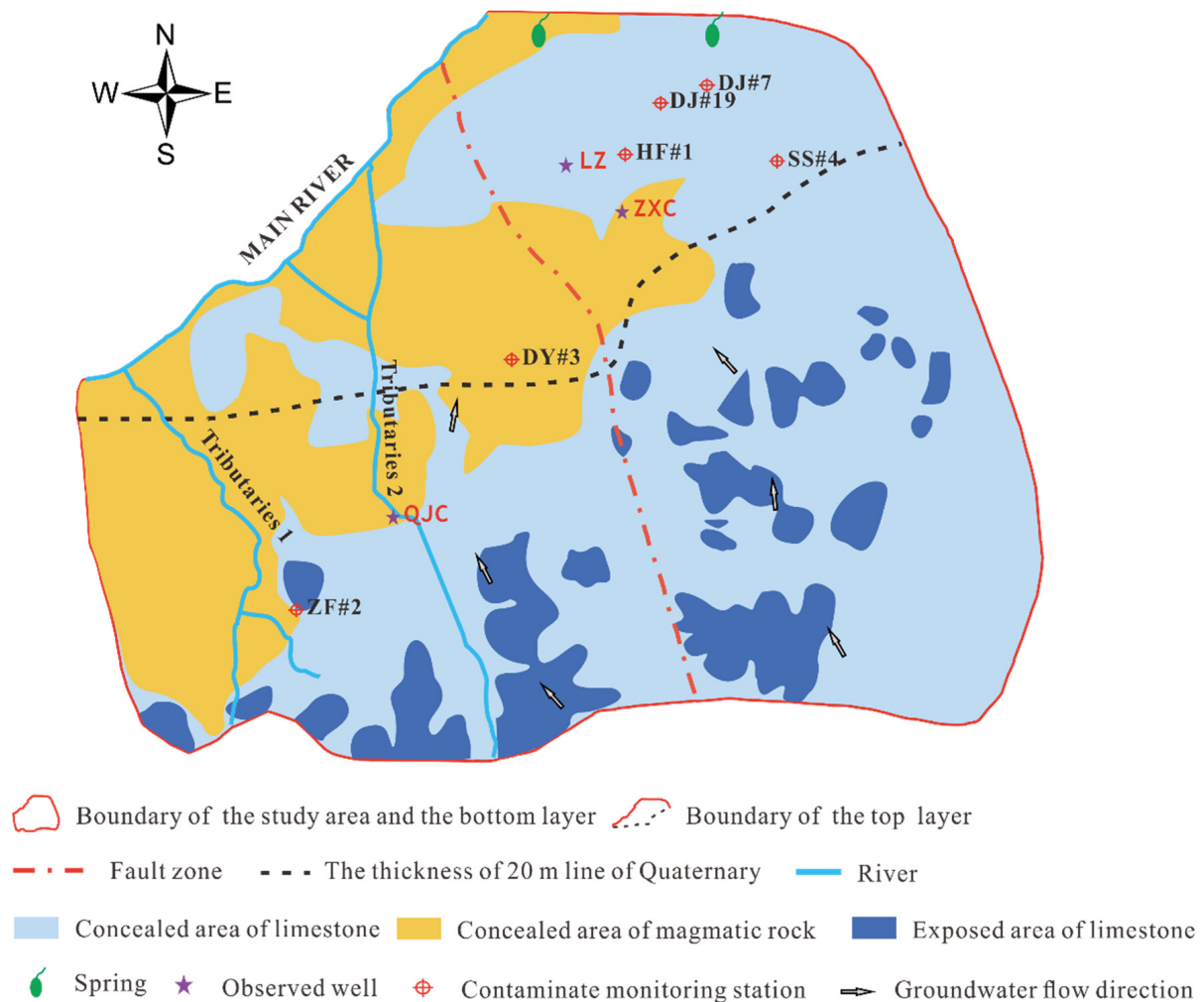

Figure 1. The location of the study area.

2.2. Factory Distribution

The northeastern part of the study area is an important industrial area, with a dense and wide distribution of factories throughout history. Since the 1970s, some fertilizer plants were set up to produce agricultural fertilizers such as ammonium chloride. Some steelworks were used to produce light-solvent oil and benzene-series products. A machine-tool plant was used to produce and clean machine parts. A textile mill needed to use rubber solvents and resin solvents in its production. Some petrochemical works produced gasoline and diesel oil. In addition, there have been cement mills, brickyards, plastic factories, chemical works and other factories in the study area. CCL4 was used or formed in the production and processing of these industrial products. The residual CCL4 on the plant surface infiltrates easily through the loose layer and enters the karst aquifer with the rainfall, resulting in serious pollution problems. Therefore, these factories are a major source of CCL4 pollution.

2.3. Field Investigation

A field investigation was conducted in the study area. A total of 151 water samples were collected, including 68 samples in the dry season and 83 samples in the wet season. Water samples were detected using the gas chromatography/mass spectrometry method. Gas chromatography is based on the fact that different substances in the solid phase and liquid phase have different partition-coefficients, so that different compounds from the column outflow-time are not the same, to achieve the purpose of separating compounds. Mass spectrometry is based on the use of the motion law of charged particles in the magnetic field or electric field, according to the mass-to-charge ratio, to achieve separation analysis and to determine the mass and intensity-distribution of ions. In 2012 and 2016, the positions that exceed the criteria are located at HF#1, DJ#19, DJ#7, SS#4, DY#3, and ZF#2, as shown in Figure 1.

2.4. Groundwater Modeling

In this study, MODFLOW is used for flow simulations and MT3D is used for pollution-transport simulations. The code was run and visualized within the Groundwater Modelling System (GMS). Although there are inhomogeneous dissolution-fractures in the study area, the karst-development degree is relatively low. The groundwater surface is uniform and continuous, and the groundwater-flow movement conforms to Darcy's law. Extensive studies have shown that karst aquifers can be reasonably generalized to equivalent porous media with homogeneous anisotropy, and simulated in MODFLOW [22–24]. The three-dimensional movement of groundwater of a constant density through porous earth-material may be described by the partial differential equation:

$$S_s \frac{\partial h}{\partial t} = \frac{\partial}{\partial x}(K_{xx}\frac{\partial h}{\partial x}) + \frac{\partial}{\partial y}(K_{yy}\frac{\partial h}{\partial y}) + \frac{\partial}{\partial z}(K_{zz}\frac{\partial h}{\partial z}) + \varepsilon \; x,y,z \in \Omega$$

$$\mu \frac{\partial h}{\partial t} = K_{xx}(\frac{\partial h}{\partial x})^2 + K_{yy}(\frac{\partial h}{\partial y})^2 + K_{zz}(\frac{\partial h}{\partial z})^2 - \frac{\partial h}{\partial z}(K_Z + p) + p$$

where S_s is the specific storage of the porous material (L^{-1}); t is Time (T); h is the hydraulic head (L); K_{xx}, K_{yy} and K_{zz} are values of hydraulic conductivity along the x, y, and z coordinate axes, which are assumed to be parallel to the major axes of hydraulic conductivity (L/T); ε is a volumetric-flux-per-unit volume representing the source and sink of water (T^{-1}).

MT3D uses the velocity values calculated by MODFLOW as inputs to solve the transport equation [25]. The equation describing three-dimension solute-transport in groundwater is:

$$\frac{\partial(\theta c)}{\partial t} = \frac{\partial}{\partial x_i}(\theta D_{ij}\frac{\partial C}{\partial x_j}) - \frac{\partial}{\partial x_i}(\theta v_i c) \pm q_s c_s$$

where θ is porosity (dimensionless); c is solute concentration (mg·L^{-1}); D_{ij} is the dispersion tensor (m^2·d^{-1}); V_i is the actual pore-water flow rate (m·d^{-1}); q_s is the value of the recharge and discharge of the unit volume of the aquifer (m^3·d^{-1}) and c_s is the solution concentration at the source and sink (mg·L^{-1}).

To estimate the transport of pollutants in the aquifer, the particle-tracking post-processing program MODPATH was used. The MODPATH program was developed by the United States Geological Survey (USGS), which was designed to work with MOD-FLOW [26]. Using the MODFLOW cell-by-cell mass-balance files, the MODPATH can track through the simulated flow-field and calculate the time-related capture zones of particles representing the pollution [27]. This program does not take chemical reactions, biodegradation, and concentration changes into account; it only considers advection transport.

MODPATH assumes the validity of Darcy's law and the law of conversation of mass in the same way as MODFLOW. MODFLOW models provide the velocities at the midpoints of the cell boundaries, and MODPATH uses simple linear interpolation to compute the velocity components within the cell [28]. Since the velocity component of a particle is a known function of the coordinates of the particle, the coordinate can be calculated at any time in the future. Particles can be tracked backward in the "upstream" direction by running the particle-tracking algorithm in reverse. Backward tracking is accomplished by reversing the sign of all the velocity components and then applying the algorithm in the same way as for forwarding tracking [29].

3. Results

3.1. Model Setup and Calibration

In line with the hydrogeological data and field survey, the model of the study area is divided into two layers; the top layer is the Quaternary layer, dominated by pore water, and the southern boundary of the top layer is the thickness of the 20 m line of the Quaternary. The bottom layer is the limestone layer, dominated by fractured-karst water. The southern boundary of the bottom layer is consistent with the southern boundary of the study area. These layer boundaries are marked in Figure 1, which is discretized into a 100 m * 100 m grid in the horizontal direction. There are 5210 effective grids in the top layer and 16,401 effective grids in the bottom layer. The simulation period is set from 1 June 2002, to 1 December 2016. Each month is a stress period, with a total of 175 stress periods, and each stress period is divided into two timesteps.

In the horizontal direction, the north is the spring discharge-zone, which is generalized as the general-head boundary. The northwest is the main river, which is generalized as a boundary of the constant head. The east and west boundaries are perpendicular to the water-table contour, and there is almost no exchange, which is generalized as the zero-flow boundary. The southern boundary of the top layer can be recharged by rainfall infiltration and is generalized as the general-head boundary. The southern boundary of the bottom layer can be recharged by piedmont lateral-runoff, and is generalized as the general-head boundary, too. In the vertical direction, the top layer is a convertible aquifer and the upper boundary is a free surface that can receive precipitation recharge, agricultural-irrigation recharge, and evaporation-loss discharge. The bottom layer is a confined aquifer, and its lower boundary is an impermeable floor. There exists leakage between the convertible aquifer and the confined aquifer.

In line with the meteorological-station precipitation data from the local meteorological bureau, we divided the study area into six precipitation zones, and the precipitation-infiltration coefficient ranges from 0.2 to 0.63, gradually decreasing from south to north. The evaporation data is from the evaporation-pan experimental data and the limit of the evaporation depth is 3.5 m. There are 27 groundwater pumping-wells to irrigate wheat and corn during the growing season, with a pumping volume of about 12×10^4 m^3/d. We use the WELL module of MODFLOW to read the monthly pumping-volume data. Agricultural pumping is regarded as surface pumping, and the division is the same as the division of the precipitation-infiltration coefficient.

Groundwater-level observation data from three monitoring wells: ZXC, LZ, and QJC, were collected. The positions of the monitoring wells are shown in Figure 1. Well ZXC had the longest time-series of observed data, from July 2002 to April 2016. The data series from LZ and QJC was relatively short, from September 2015 to December 2016, and from December 2015 to December 2016, respectively. We verified the applicability of the simulation results by comparing the simulated water-level with the observed water-level of these three monitoring wells, as shown in Figure 2. We calculated the error coefficients for the three monitoring wells: the error coefficient for ZXC was 2.8%, for LZ it was 6.5%, and for QJC it was 7.14%. These error coefficients are all within 10%, which means the simulated groundwater-level was consistent with the measured groundwater-level [30].
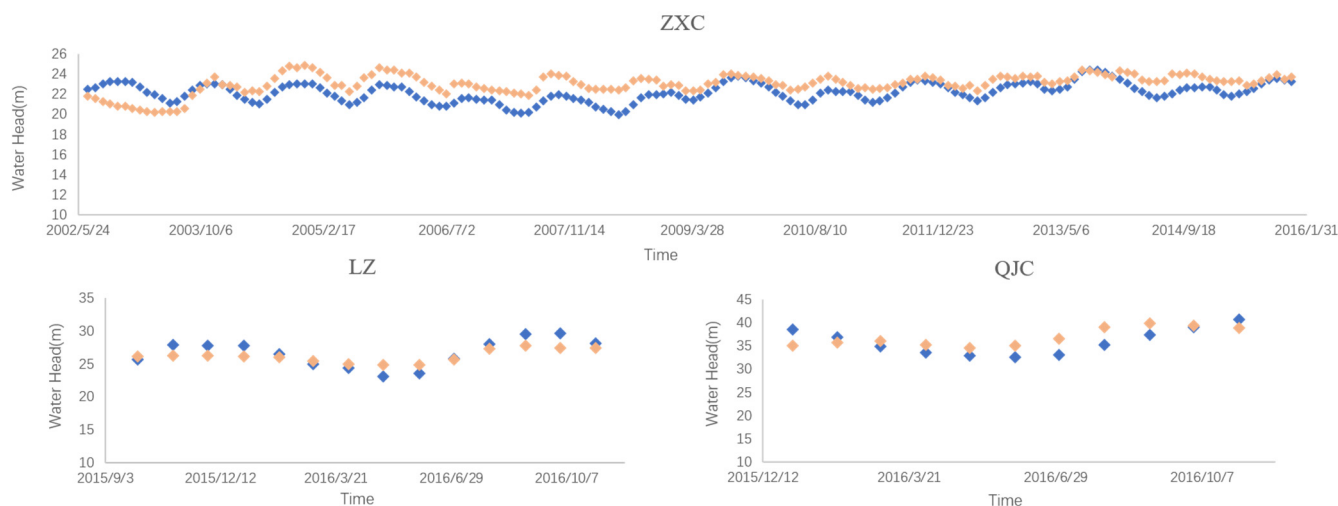

Figure 2. Comparison curve between observed water-level and simulated water-level.

In addition, we also compared the simulated flow-field in the year 2016 with the actual flow-field diagram, as shown in Figure 3. It can be seen that although there are some differences between the simulated water-levels and the observed water-levels, it conforms to the dynamic characteristics of groundwater. The groundwater flow generally flows from south to north. The hydraulic gradient of groundwater flow in mountainous areas is relatively large, and the water level is relatively dense. The hydraulic gradient in the plain area is small, and the water level is sparse. In the simulated flow-field, the groundwater-drawdown cone and fault zone are reflected.

3.2. Analysis of CCL4 Concentration

The concentration-distribution map showed the concentration range and variation trend of CCL4 in 2012 and 2016, as shown in Figure 4. In the northeast and southwest of the study area, there were two centers of pollution concentration. In 2012, the concentration center in the southwest area was near the monitoring well ZF#2, with a value of about 20 ug/L. In 2016, the concentration center in the southwest had barely changed, with a central concentration decrease of about 15 ug/L. In the northeast area, the highest concentration of CCL4 was about 25 ug/L, in the year 2012. By 2016, the concentration center had shifted to the south, near the monitoring well HF#1, and the concentration was around 35 ug/L. There was an area near the monitoring well DY#3 where CCL4 concentrations were around 2 ug/L in both 2012 and 2016.
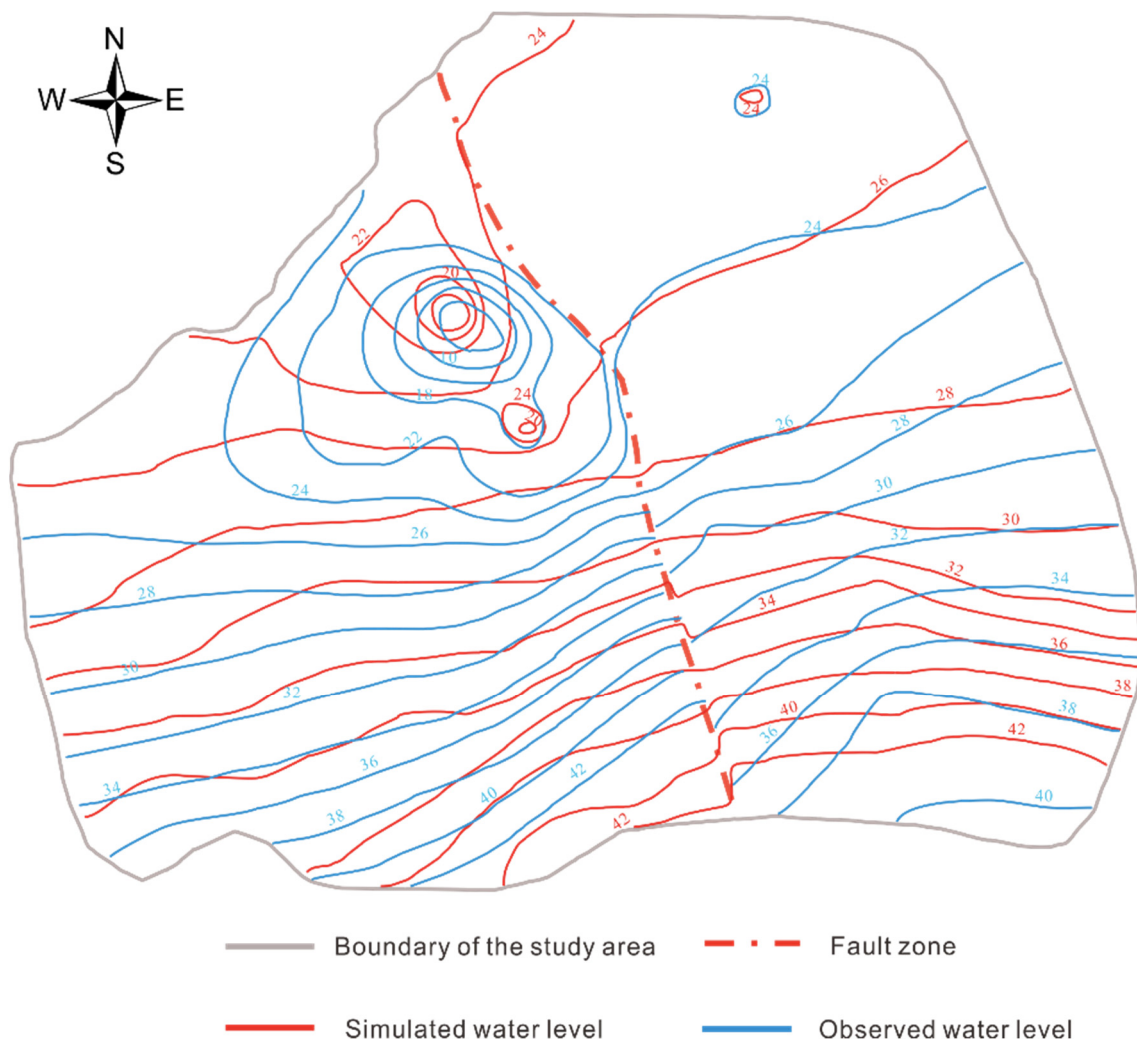
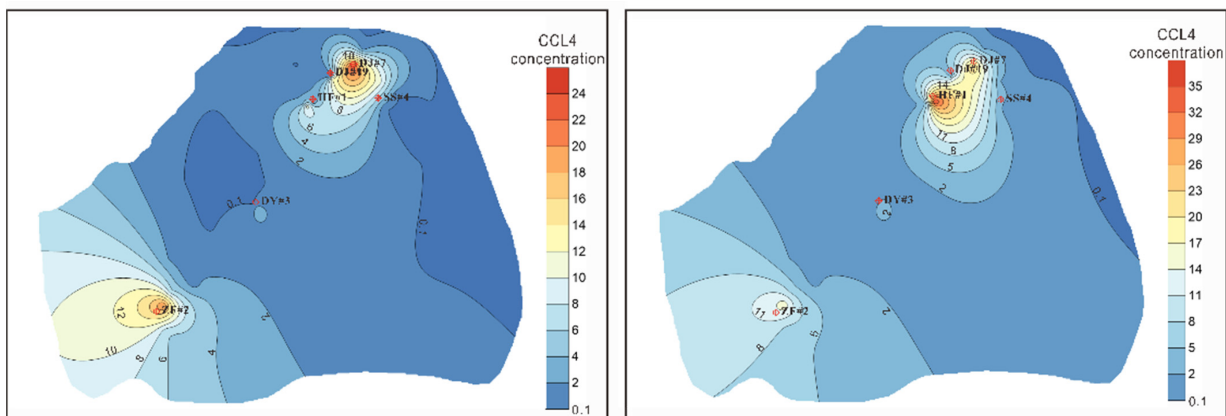**Figure 3.** Diagram of the simulated flow-field and observed flow-field in 2016.

Figure 4. CCL4 concentration distribution map in 2012 (**left**) and 2016 (**right**).

According to the distribution map, parts of the river segment have been affected by CCL4 pollution in the southern area. Compared with the northeast, the pollution scope in the southwest is larger, but the concentration in the center is smaller. In the northwest, a large area of contamination has formed around the monitoring well HF#1-DJ#7-DJ#19-SS#4, which is adjacent to the historic industrial area, and which is largely attributable to

industrial pollution. With the flow of groundwater, the scope of pollution continues to expand, threatening the quality of rivers and springs. It is necessary to carry out backward tracing of CCL4 pollution, to delineate the location of the pollution source and control the diffusion of pollutants.

3.3. Backward Tracing of the Polluted Zone

We used MODPATH to carry out the backward particle-trace and capture the pollution zone for the past 30 years and 50 years, respectively, to obtain the possible location of the potentially polluted factories.

According to where the CCL4 pollution was detected in 2012 and 2016, we placed the particles at the location of HF#1, DJ#19, DJ#7, SS#4, ZF#2, and DY#3. Restricted by detection conditions, the location of these polluted points may not be the real center of pollutant concentration. Therefore, with the detected point as the center, the particles were placed in the surrounding area of 250 m. The particle-tracing duration was 30 years, from January 1987 to December 2016, and 50 years, from January 1967 to December 2016, to investigate the potential pollution-factories in the 1990s and 1970s, as shown in Figures 5 and 6. Due to the data required by the model before 2002 being missing, the steady-flow simulation was carried out before the year 2002, and the transient-flow simulation was carried out in the model from the year 2002 to 2016.
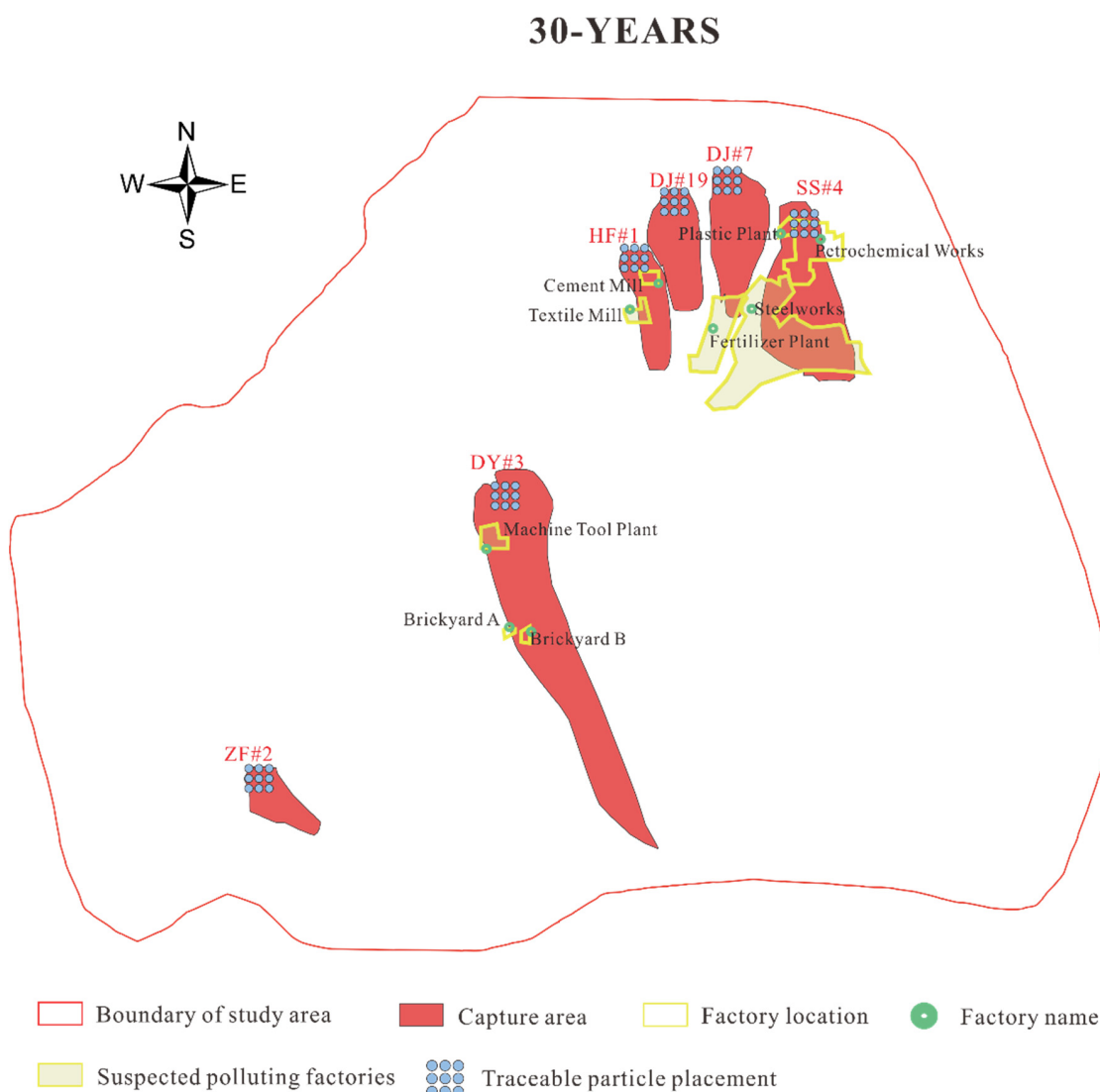

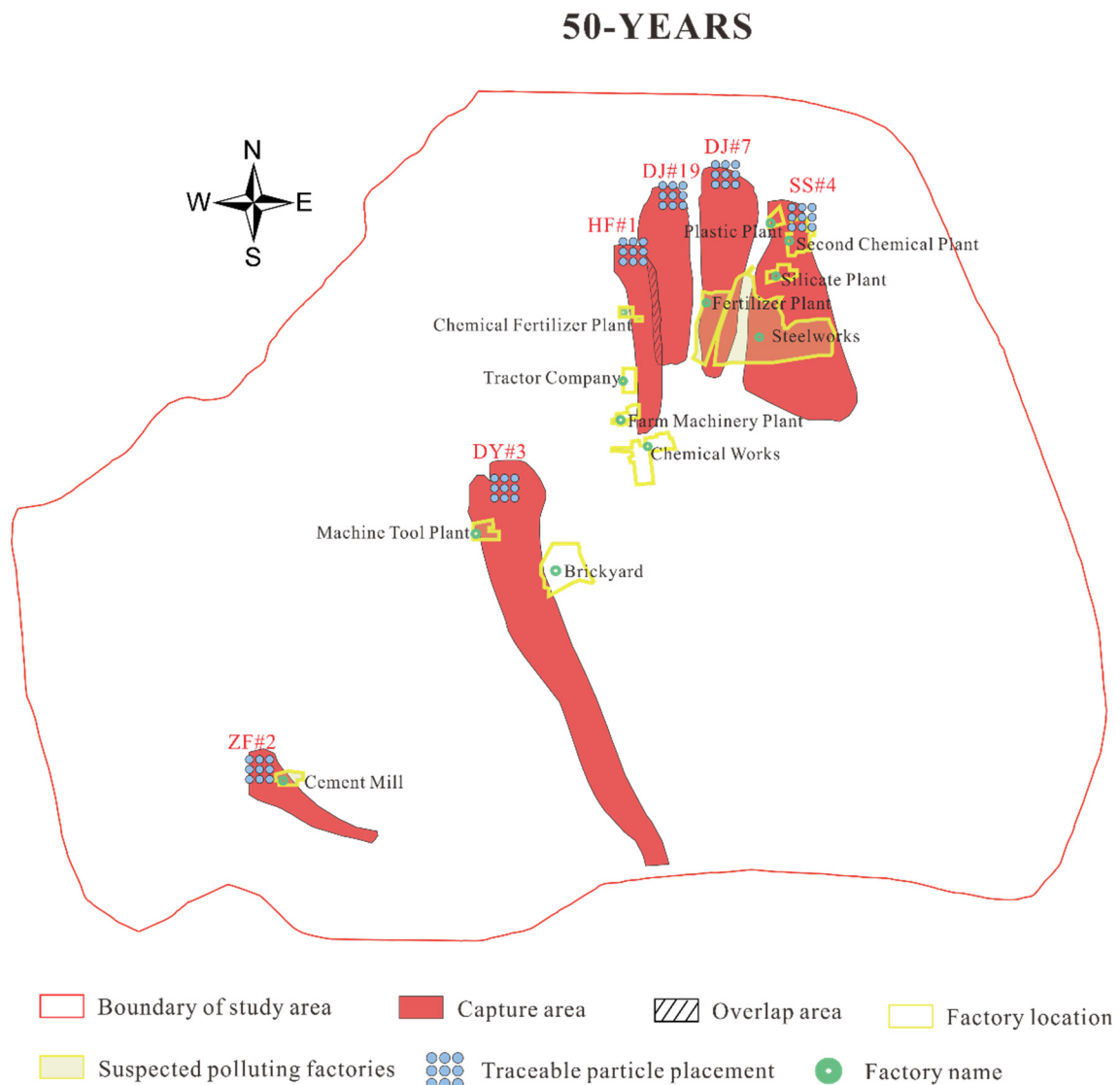**Figure 5.** Pollution zone captured in the 1990s (30 years ago).

50-YEARS

Figure 6. Pollution zone captured in the 1970s (50 years ago).

The results of the 30-year backward tracing are shown in Figure 5. Table 1 shows the areas of pollutant ranges of the six pollution-detected points in the 1990s. The captured zone around HF#1 was about 1900 m long and 500 m wide, and there was a cement mill and textile mill that existed in the 1990s. The captured area around DJ#19 was about 1800 m long and 700 m wide, but there was no historical factory in its capture zone. There was no intersection between the polluted areas captured between HF#1 and DJ#19. The captured zone around DJ#7 was about 2300 m long and 800 m wide, and a fertilizer plant existed. The captured zone around SS#4 was about 2700 m long and 1000 m wide, and the historical factories in the capture zone were the plastic plant and fertilizer plant. The captured area around DY#3 was about 6200 m long and 800 m wide; within the capture zone, there were two brickyards and a machine-tool plant. The area of ZF#2 was the smallest, and there was no historical factory in ZF#2's capture zone. The capture zone of DY#3 was much larger than the other places, because the hydrogeological conditions of DY#3 are favorable for groundwater flow, and with the existence of a water-supply company, the amount of water pumping in the DY#3 area is considerable. Combined with the products produced by these factories, in the 1990s the potential polluting factories were the textile mill, fertilizer plant, steelworks, and machine-tool plant.

Table 1. Area of pollution-range captured by 6 pollution-detected points in the 1990s.

Well Name	ZF#2	DY#3	HF#1	DJ#19	DJ#7	SS#4
Capture area (km^2)	0.62	4.43	0.88	1.46	1.13	2.60

The results of the 50-year backward tracing are shown in Figure 6. Table 2 shows the areas of pollutant ranges of the six pollution-detected points in the 1970s. The capture zone of each monitoring well has increased, especially the capture zone of DY#3, which has exceeded the southern boundary. Within its capture zone there was a machine-tool plant and a brickyard in the 1970s. An overlapping area occurred between the capture zones of HF#1 and DJ#19, but the overlapping part had no factory in the 1970s. The captured zone around HF#1 was about 3000 m long and 450 m wide. In the 1970s, there was a chemical-fertilizer plant in the capture zone, and there was a tractor company, a farm machinery plant, and a chemical works in the vicinity. There was no historical factory in DJ#19's capture zone, and a fertilizer plant existed in DJ#7's capture zone. The factories that existed within the capture zone of SS#4 were a plastic plant, a second chemical plant, a silicate plant, and steelworks. There was a cement mill in the capture zone of ZF#2 in the 1970s. Combined with the products produced by these factories, in the 1970s the potential polluting factories were the chemical-fertilizer plant, the fertilizer plant, the steelworks, the machine-tool plant, and the cement mill.

Table 2. Area of pollution range captured by 6 pollutions detected points in the 1970s.

Well Name	ZF#2	DY#3	HF#1	DJ#19	DJ#7	SS#4
Capture area (km^2)	0.88	>4.77	1.27	2.12	1.72	3.90

3.4. Forward Simulation of CCL4 Transport

By backward tracing, we identified a number of potential polluted factories within the capture zone. To further pinpoint the location of the polluting factories, we performed forward solute-transport at the location of these potential polluted factories, and compared the simulated concentration of forwarding simulation with the observed concentration-data.

Two scenarios were set up, assuming that CCL4 leaks occurred in the 1970s and 1990s. Based on the existing flow-model (transient flow from 2002 to 2016 and steady flow before 2002), the forward solute-transport simulation was carried out. The release of pollutants was instantaneous, without subsequent replenishment. The initial concentration was 785 mg/L, and this value is the solubility of CCl4 in water at 25 °C. Potentially polluting factories are located in the Quaternary layer or the limestone layer, with the parameters related to solute transport in these two layers shown in Table 3.

Table 3. Pollutant-transport parameters of the Quaternary layer and the limestone layer.

	Longitudinal Dispersion	Transverse Dispersion	Molecular Diffusivity
Quaternary	1 m	0.16 m	1.57×10^{-7} m^2/d
Limestone	1.48 m	0.26 m	1.75×10^{-7} m^2/d

Scenario 1: Assuming that the source of pollutant leakage was factories in the 1990s. Potentially polluting factories are the textile mill, the fertilizer plant, the steelworks, and the machine-tool plant. We put pollution particles where these factories were located; among them, the placements of the textile mill and the fertilizer plant were in the Quaternary layer, and the steelworks and machine-tool plant were in the limestone layer. The simulation started in the year 1987. The distribution range of pollutants in August 2012 and October 2016 is shown in Figure 7.
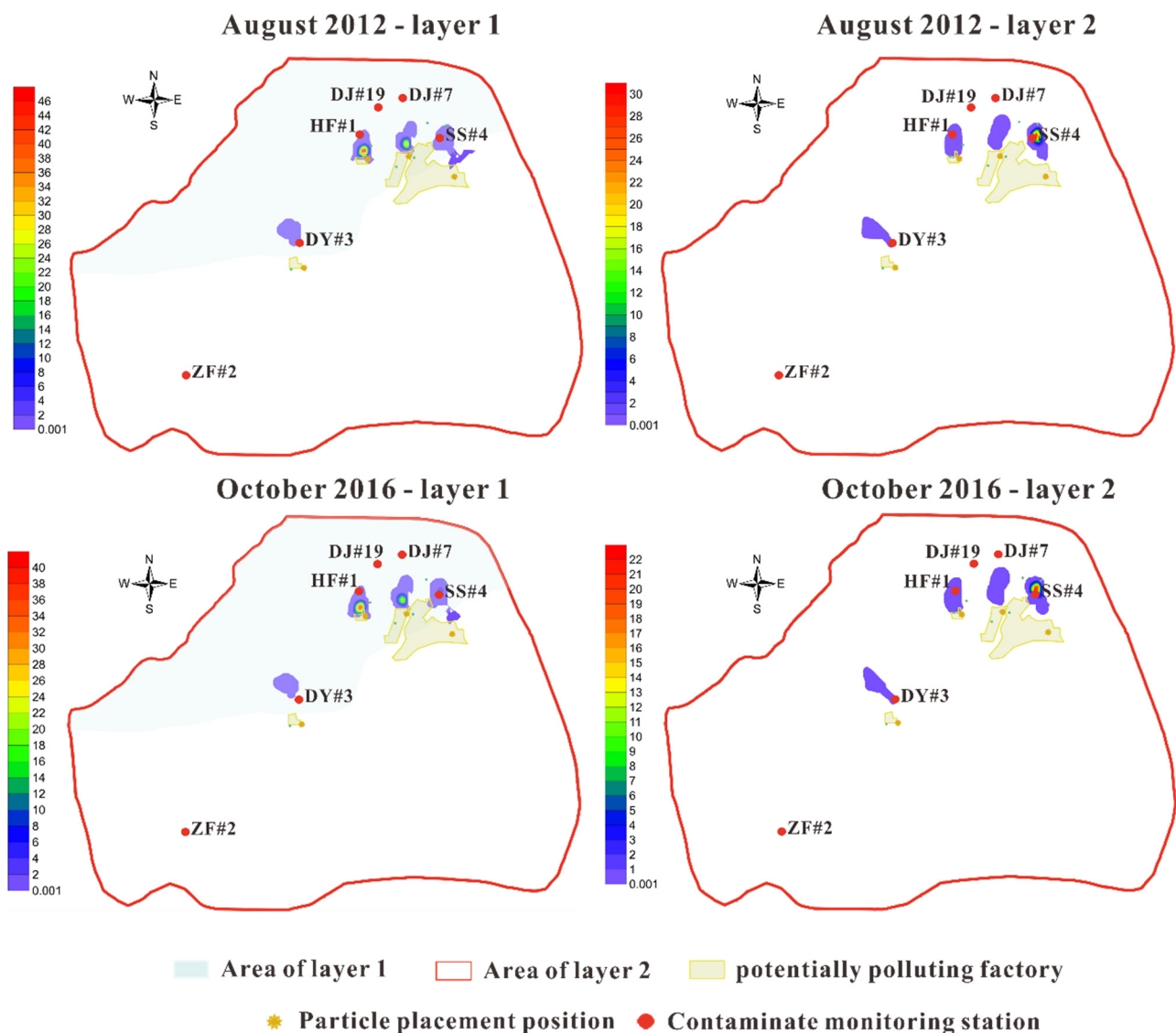
Figure 7. Pollutant-concentration distribution in August 2012 and December 2016 in Scenario 1.

The Quaternary layer is also layer 1 of the model. In August 2012, the concentration of CCL4 at 200 m distances from the textile mill was the highest, at 47 mg/L. As it is 300 m away from the fertilizer plant, the CCL4 concentration was 27 mg/L. The concentration near the steelworks was 2.24 mg/L. CCL4 appeared at a distance of 1500 m from the machine-tool plant, with a concentration of about 0.85 mg/L. The concentration of CCL4 in the textile mill and fertilizer plant was higher, and the distance from the particle placement-point was closer. In October 2016, compared with August 2012, the concentration of CCL4 did not change much, and the distribution range maintained the original form. The highest concentration was still 200 m away from the textile mill, but the concentration was slightly reduced, to 43 mg/L.

The limestone layer is also layer 2 of the model. In August 2012, the highest-concentration point appeared at 2000 m from the steelworks, at 30 mg/L. The CCL4 concentration of other polluted areas was around 0.05 mg/L. In October 2016, compared with August 2012, the highest concentration in the steelworks was reduced to 22 mg/L, and the distribution of CCL4 did not change much. In general, CCL4 in limestone layers transports faster than in the Quaternary layer.

Scenario 2: Assuming that the source of pollutant leakage was factories in the 1970s. Potentially polluting factories are the chemical-fertilizer plant, the fertilizer plant, the

steelworks, the machine-tool plant, and the cement mill. We put pollution particles where these factories are located, and among them, the placement of the chemical-fertilizer plant and the fertilizer plant were in the Quaternary layer, and the steelworks, machine-tool plant, and cement mill were in the limestone layer. The simulation started in the year 1967. The distribution range of pollutants in August 2012 and October 2016 is shown in Figure 8.
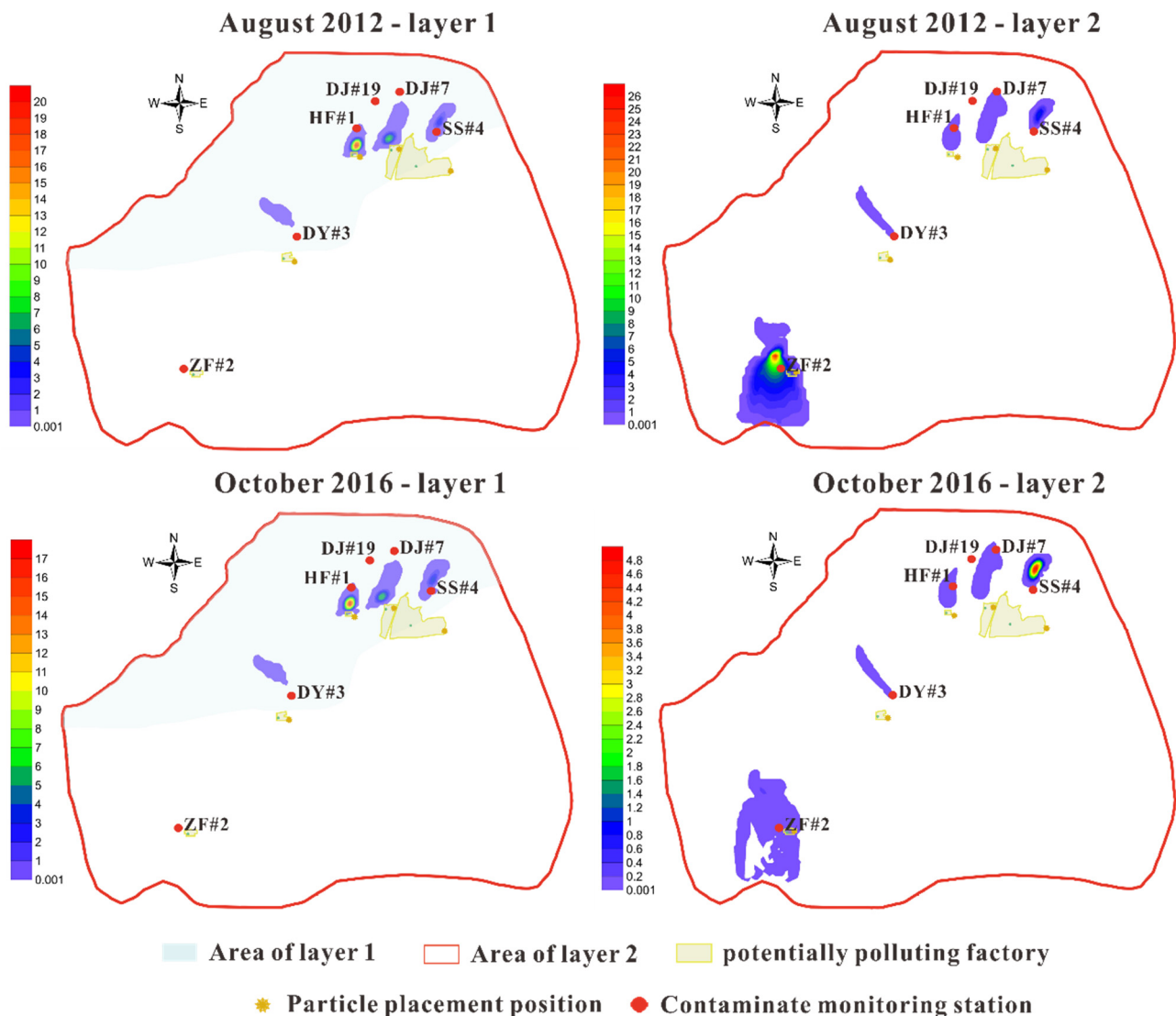

Figure 8. Pollutant-concentration distribution in August 2012 and December 2016, in Scenario 2.

The Quaternary layer is also layer 1 of the model. In August 2012, the concentration of CCL4 in the chemical-plant area was the highest, at 20 mg/L. In the north of the fertilizer plant, the CCL4 concentration was 8 mg/L. At 2500 m from the steelworks, the concentration of CCL4 was 4 mg/L. The concentration near the machine-tool plant was 2.24 mg/L. In October 2016, compared with August 2012, the concentration of CCL4 slightly decreased, and the distribution range maintained its original form.

The limestone layer is also layer 2 of the model. In August 2012, the highest-concentration point appeared at 1000 m from the cement mill, and reached 26 mg/L. The distribution range was large, which is associated with frequent groundwater head-dynamics in this area. In October 2016, compared with August 2012, the maximum CCL4 concentration point changed from the machine-tool-plant area to the steelworks area. The highest concentration near the steelworks was 4.8 mg/L.

3.5. Characteristics of CCL4 Transport

The observed concentrations of CCL4 pollution in HF#1, DJ#19, DJ#7, SS#4, ZF#2, and DY#3 in the years 2012 and 2016 are shown in Table 4 Comparing the simulated- and observed-concentration, in 2012 at point HF#1, regardless of whether it were Scenario 1 or Scenario 2, the simulated concentration of layer 1 was closer to the observed value, and layer 2 was slightly higher. Meanwhile, in 2016 it was the opposite: layer 2 was closer to the observed value, and the concentration value of scenario 1 was 34.36 ug/L in the year 2016, which was almost consistent with the observed value. This indicates that the textile mill is more likely to be a potential source of CCL4 pollution. The steelworks in both Scenario 1 and Scenario 2 are at point SS#4, but the simulated concentration value of Scenario 1 was high, and the concentration of Scenario 2 was significantly decreased, especially the concentration of layer 1 in 2016, which was almost the same as the observed concentration. This difference may be related to the high initial concentration at the particle-delivery point. The difference between the simulated concentration at DY#3 and the observed value was relatively small, especially in Scenario 1, which was the same as the observed value in 2016, which means that the machine-tool plant is likely to be a source of pollution. Since there are no potentially polluting factories at DJ#19 and no factory at ZF#2 for Scenario 1, no pollution was simulated during the simulation period. In Scenario 2, the simulated CCL4 value was very high at ZF#2, far exceeding the observed value. It can be inferred that the pollution detected at DJ#19 and ZF#2 may not be caused by a leak from factories in their pollution-capture zone, but by the superposition of pollutants in other areas. No matter which scenario it is, the pollution at DY#3 transports faster, about 130 m/year. The pollution-transport speed at ZF#2 was the slowest, about 30 m/year. In the HF#1-DJ#19-DJ#7-SS#4 region, the pollution-transport speed was about 50 m/year.

Table 4. The concentrations of CCL4 pollution at detected points in the year 2012 and 2016 (units: ug/L).

Factory Name	August 2012					October 2016				
	Observed	Scenario 1		Scenario 2		Observed	Scenario 1		Scenario 2	
		Layer 1	Layer 2	Layer 1	Layer 2		Layer 1	Layer 2	Layer 1	Layer 2
HF#1	3.07	2.05	8.82	2.74	10.53	35.43	1.69	34.36	5.13	15.03
DJ#19	0. 64	-	-	-	-	11.67	-	-	-	-
DJ#7	-	-	-	-	1.33	23.6	-	-	-	16.8
SS#4	10.39	82	8301	1.22	232.5	1.77	498.6	6651	1.76	13.34
ZF#2	20.22	-	3690	-	-	15.8	-	20.59	-	-
DY#3	1.19	2.0	4.4	-	5.75	3.08	-	3.08	-	1.88

In order to further analyze the pollutant transport, the simulated concentration–duration curve at the monitoring well near the pollution source is drawn.

By analyzing the concentration–duration curve of the HF#1 well near the textile mill since 1986 (Figure 9), it can be found that the pollutants are mainly located in layer 2, which is limestone aquifer. The simulated concentration of HF#1 shows a gradual upward trend. The simulated concentration is close to the observed concentration in 2016, but the concentration in 2012 is much higher than the observed concentration. The observed concentration also shows an upward trend, and it can be speculated that the pollution is still in the rising period, that is, pollution may occur after 1986, or closer to the detection point.

By analyzing the concentration–duration curve of the SS#4 well near the steelworks since 1966 (Figure 10), it can be found that the pollutant concentration in layer 2 is higher, and the migration speed is faster. Compared with the observed concentration, the simulated concentration of the layer 2 is significantly higher, while the concentration of layer 1 is closer to the observed value. It can be inferred that the pollutants may diffuse through the Quaternary aquifer. As the simulated value of the layer 1 is slightly lower than the observed value, the pollutant-leakage time should be slightly later than the year 1966.
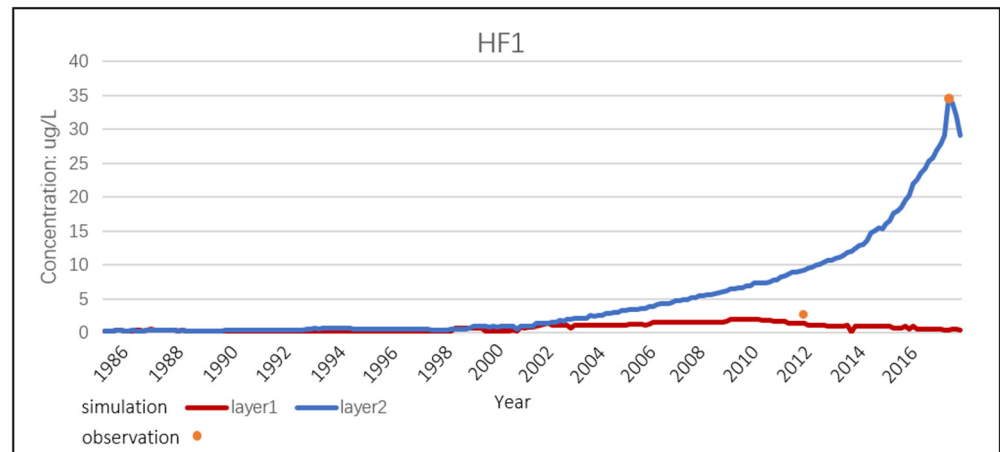
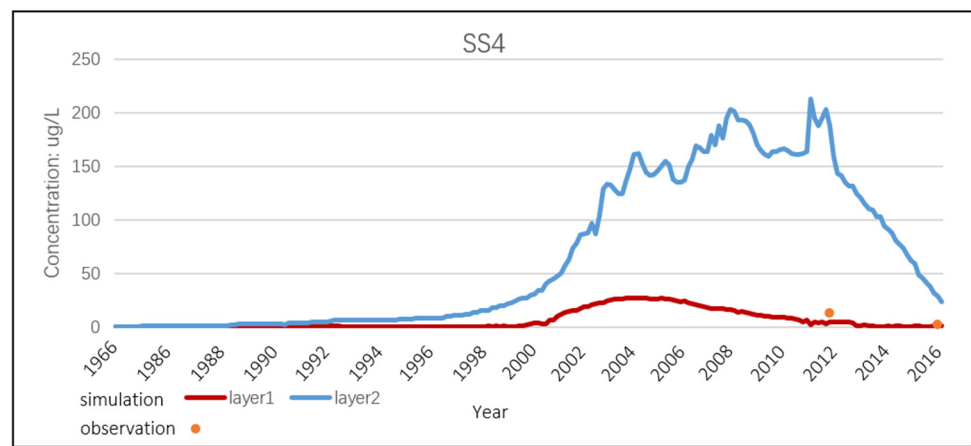**Figure 9.** CCL4 concentration– duration curve of the HF#1 well.

Figure 10. CCL4 concentration–duration curve of the SS#4 well.

The machine-tool plant is located on the limestone aquifer, and its pollutants migrate in layer 2. By analyzing the concentration–duration curve of the DY#3 well near the machine-tool plant (Figure 11), it can be found that whether the pollution leakage occurred in 1966 or 1986, the peak value will appear after a period of time, and the peak shape is similar. Compared with the simulated concentration, the observed concentration in 2012 and 2016 show little difference between Scenario 1 and Scenario 2. Therefore, it is inferred that both scenarios may be pollution-source years.
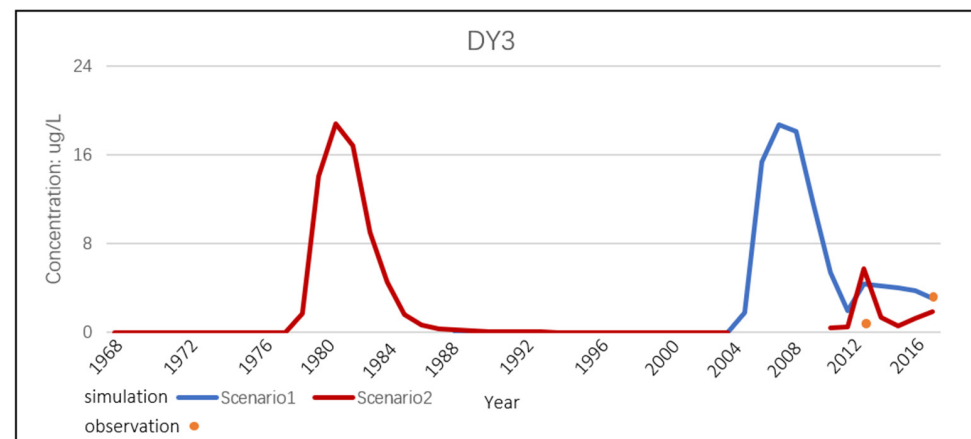

Figure 11. CCL4 concentration duration curve of the DY#3 well.

4. Discussion

Large-scale use of CCL4 will cause significant environmental soil and groundwater contamination, resulting in great health-risks, such as carcinogenic, teratogenic, and mutagenic effects, and can damage the human central nervous system, liver organs, and kidneys [6]. Therefore, it is important and urgent to control carbon tetrachloride pollution in groundwater.

In previous studies in the study area, due to insufficient hydrochemical data, based on solely hydrochemical analysis it was impossible to effectively delineate the zone of pollution sources. The complex hydrogeological conditions in the study area and the existence of fault zones made it impossible to trace the source of pollutants using the isotope method. As a result, tracing the source of CCL4 pollutants has been a major problem for a long time.

The most commonly used numerical-simulation method to trace the source of pollution is the MODPATH tool. There are some research cases; for example, Alberti, L et al. applied the MODPATH code to generate back-traced advective-flow paths to find multiple-point sources of groundwater pollution [15]. Lazzaroni, M et al. used the MODFLOW computer program to identify where the source of contamination is likely located [16]. However, this method only uses MODPATH to trace the source, which is more applicable to cases where the location of pollution sources is relatively clear or the pollution investigation is very detailed. In our study area, the tracing time-span is very large and the long-term observation data of pollutants is scarce. If we only use MODPATH, the delineated pollution range will be very uncertain. In addition, if every contaminated well is traced, the problem of multiple point-sources will be generated, which is not conducive to the development of traceability work.

In this work, we adopted the method of combining hydrochemical analysis, backward tracing, and forward simulation, to trace the source of pollutants. Through hydrochemical analysis, the locations of typical contaminated wells were screened out through the concentration field. Contamination in these typical wells is caused by CCL4 leakage and transport, and these wells are helpful in accurately tracing the source. MT3D has many applications in pollutant transport; for example, Guo Ying et al. analyzed the form of the contaminant plume as well as the changing features under the influence of multiple factors [31]. M Wen et al. established a solute-transport model based on the sampled data to predict carbon tetrachloride pollution in the study area over the next 15 years [18]. Islam, MR et al. simulated CCL4 contaminant plumes in the aquifer with MT3D and observed the dynamic equilibrium of the plume after approximately 12 years, assuming constant sources [32]. These works are of great significance, but they focus more on analyzing and predicting the transport of pollutants, without considering the traceability of pollutants. In our research area, the forward-transport simulation of MT3D is used in the traceability work. On the one hand, it is combined with backward tracing to further determine the specific location of the pollution source, so as to reduce uncertainty. On the other hand, it is helpful to analyze the characteristics of pollutant transport, to determine the pollution layer and pollutant-transport speed.

5. Conclusions

In this work, we established a traceability-method system by combining hydrochemical analysis, backward tracing, and forward transport, and successfully delineated the source of CCL4 pollution in an eastern city of China.

The CCL4 concentration-field in the ear 2012 and 2016 showed that in the northeast and southwest of the study area, there were two centers of pollution concentration. In the middle of the study area, there is a small regional-pollution center, where CCL4 is about 2 ug/L. These pollution centers were caused by CCL4 leakage and transport. Six monitoring wells: HF#1, DJ#19, DJ#7, SS#4, ZF#2, and DY#3 are located in the contaminated center, and exceed the CCL4-concentration criteria.

Using MODPATH for backward tracing, we delineated the pollution zone of six CCL4-pollution-detected points: HF#1, DJ#19, DJ#7, SS#4, ZF#2, and DY#3 30 years ago (the

1990s) and 50 years ago (the 1970s). The results showed that the capture zone of DY#3 is the largest, being 4.43 km^2 in the 1990s and exceeding 4.77 km^2 in the 1970s, and the potential polluting factory in its capture zone was the machine-tool plant. The potential polluting factory was the textile mill and the chemical-fertilizer plant in HF#1′s area, the fertilizer plants in DJ#7′s area, the steelworks in SS#4′s area, and the cement mill in the 1970s in ZF#2′s area.

We performed forward simulations and set Scenario 1: delivery of pollutant particles to potentially polluting factories in the 1990s. Scenario 2: delivery of pollutant particles to potentially polluting factories in the 1970s. By comparing the simulated concentration with the observed concentration, we infer that the textile mill in 1990s, the steelworks in the 1970s, and the machine-tool plant in the 1970s and 1990s are likely to be the source of pollution, and the contaminants at ZF#2 and DJ#19 are likely to be generated by the migration or superposition of pollutants in other areas. The contaminant-transport speed at DY#3 was 130 m/year, while at ZF#2 it was 30 m/year. In the HF#1-DJ#19-DJ#7-SS#4 region, the pollution-transport speed was about 50 m/year.

By analyzing the concentration–duration curve of HF#1, SS#4, and DY#3 wells near the pollution source, it can be found that CCL4 in limestone layers transports faster than in the Quaternary layer. The pollutant in the textile mill was from the limestone layer, and was released slightly later than 1986. The pollutant at the steelworks originated from the Quaternary layer, and was released slightly later than 1966.

This study delineated the contaminated zone of CCL4 and provided a possible source of CCL4, which helps to further identify the contamination source and remediate pollutants. However, the pollution-concentration observed data is lacking, leading to the pollution-transport simulation results showing uncertainty. In addition, the exact us-ime and pollution-storage location in the factories need further investigation.

Author Contributions: Conceptualization, B.G.; data curation, H.A. and Y.L.; investigation, P.Y. and H.A.; methodology, B.G. and X.L.; supervision, P.Y. and R.K.; visualization, Y.Z. and Y.L.; writing—original draft, B.G. and Y.Z. All authors have read and agreed to the published version of the manuscript.

Institutional Review Board Statement: Not applicable.

Informed Consent Statement: Not applicable.

Data Availability Statement: The datasets generated and analyzed during the current study are available from the corresponding author upon reasonable request.

Conflicts of Interest: The authors declare no conflict of interest.

References

1. Rathi, B.S.; Kumar, P.S.; Show, P.L. A review on effective removal of emerging contaminants from aquatic systems: Current trends and scope for further research. *J. Hazard. Mater.* **2021**, *409*, 124413. [CrossRef] [PubMed]
2. Stuart, M.; Lapworth, D.; Crane, E.; Hart, A. Review of risk from potential emerging contaminants in UK groundwater. *Sci. Total Environ.* **2012**, *416*, 1–21. [CrossRef] [PubMed]
3. Liang, Z.; Han, B.; Jie, M.A.; Liang, X.; Liu, X.; Zhao, H.; Weili, W.U.; Qiu, C.; Xiao, Y. Simulation on Treatment of Carbon Tetrachloride in Groundwater with Bimetal Dielectric Chemical Reaction Wells. *Environ. Sci. Technol.* **2014**, *37*, 141–146.
4. Penny, C.; Gruffaz, C.; Nadalig, T.; Cauchie, H.M.; Vuilleumier, S.; Bringel, F. Tetrachloromethane-Degrading Bacterial Enrichment Cultures and Isolates from a Contaminated Aquifer. *Microorganisms* **2015**, *3*, 327–343. [CrossRef]
5. Doherty, R.E. A History of the Production and Use of Carbon Tetrachloride, Tetrachloroethylene, Trichloroethylene and 1,1,1-Trichloroethane in the United States: Part 1–Historical Background; Carbon Tetrachloride and Tetrachloroethylene. *Environ. Forensics* **2000**, *1*, 69–81. [CrossRef]

6. Liu, D.; Liu, B.; Zhan, H. The Health Risk Assessment of CCl_4 in groundwater of a Certain Chemical Plant. *IOP Conf. Ser. Earth Environ. Sci.* **2018**, *153*, 052011. [CrossRef]

7. Sautter, S. BHI ERC team zeroes in on sources of carbon tetrachloride contamination Hanford Rench. *Hanford Rench March* **2001**, *19*, 1–17.

8. Skrökki, A. Quality of drinking water from one surface water plant and six groundwater plants in the town of Kajaani in Finland. *Vatten* **1992**, *48*, 78–81.

9. Jiang, P.; Ma, Z.M.; Yu, W.W.; Wen, M. Carbon tetrachloride pollution pathway of groundwater a typical contaminated site in the east of the city. *IOP Conf. Ser. Earth Environ. Sci.* **2017**, *82*, 012058. [CrossRef]

10. Datta, B.; Prakash, O.; Cassou, P.; Valetaud, M. Optimal Unknown Pollution Source Characterization in a Contaminated Groundwater Aquifer—Evaluation of a Developed Dedicated Software Tool. *J. Geosci. Environ. Prot.* **2014**, *2*, 11. [CrossRef]

11. Wang, H.; Shi, Z.; Jiang, Y.; Lian, X.; Yang, Y.; Feng, F.; Jia, Y. Research Progress on Indicator of Groundwater Pollution Identification and Traceability. *Res. Environ. Sci.* **2021**, *34*, 1886–1898.

12. Mansuy, L.; Philp, R.P.; Allen, J. Source identification of oil spills based on the isotopic composition of individual components in weathered oil samples. *Environ. Sci. Technol.* **1997**, *31*, 3417–3425. [CrossRef]

13. Atmadja, J.; Bagtzoglou, A.C. State of the art report on mathematical methods for groundwater pollution source identification. *Environ. Forensics* **2001**, *2*, 205–214. [CrossRef]

14. Gu, X.; Shao, J.; Cui, Y.; Hao, Q. Calibration of two-dimensional variably saturated numerical model for groundwater flow in arid inland basin, China. *Curr. Sci. A Fortn. J. Res.* **2017**, *113*, 403–412. [CrossRef]

15. Banejad, H.; Mohebzadeh, H.; Ghobadi, M.H. Numerical Simulation of Groundwater Flow and Contamination Transport in Nahavand Plain Aquifer, West of Iran. *J. Geol. Soc. India* **2014**, *83*, 83–92. [CrossRef]

16. Alberti, L.; Colombo, L.; Formentin, G. Null-space Monte Carlo particle tracking to assess groundwater PCE (Tetrachloroethene) diffuse pollution in north-eastern Milan functional urban area. *Sci. Total Environ.* **2018**, *621*, 326–339. [CrossRef]

17. Lazzaroni, M.; Ceccatelli, M.; Rossato, L.; Nisi, B.; Venturi, S.; Fanti, R.; Tassi, F.; Vaselli, O. Boron pollution in the shallow groundwater system from Isola di Castelluccio (central-eastern Tuscany): Evidences from a geochemical survey and new remediation perspectives from a recently-installed hydraulic barrier and hydrogeological modelling. *Ital. J. Geosci.* **2021**, *140*, 121–140. [CrossRef]

18. Zhang, S.; Ma, Z.; Liu, S. Numerical simulation and prediction of chlorinated hydrocarbon migration in eastern Jinan. *IOP Conf. Ser. Earth Environ. Sci.* **2020**, *531*, 012028. [CrossRef]

19. Wen, M.; Ma, Z.; Jiang, p.; Yu, W. Study on the Law of Carbon Tetrachloride Migration in Groundwater System. In Proceedings of the 2017 2nd International Conference on Advanced Materials Science and Environment Engineering(AMSEE2017), Sanya, China, 25 June 2017; pp. 214–219.

20. Eryigit, M.; Engel, B. Spatiotemporal Modelling of Groundwater Flow and Nitrate Contamination in An Agriculture-Dominated Watershed. *J. Environ. Inform.* **2022**, *39*, 125–135. [CrossRef]

21. Ayvaz, M.T. A hybrid simulation–optimization approach for solving the areal groundwater pollution source identification problems. *J. Hydrol.* **2016**, *538*, 161–176. [CrossRef]

22. Wei, J.; Guo, Y.; Wang, R.; Jiang, Y. Recent advances in simulation approaches of the complex karst medium. *Hydrogeol. Eng. Geol.* **2015**, *42*, 23–34.

23. Abdelaziz, R.; Bambi, C.K.M. Groundwater Assessment of the Bleleone Catchment Karst Aquifer in Southern France. In Proceedings of the World Multidisciplinary Earth Sciences symposium (WMESS), Prague, Czech Republic, 5–9 September 2016.

24. Baalousha, H.M.; Fahs, M.; Ramasomanana, F.; Younes, A. Effect of Pilot-Points Location on Model Calibration: Application to the Northern Karst Aquifer of Qatar. *Water* **2019**, *11*, 679. [CrossRef]

25. Lautz, L.K.; Siegel, D.I. Modeling surface and ground water mixing in the hyporheic zone using MODFLOW and MT3D. *Adv. Water Resour.* **2006**, *29*, 1618–1633. [CrossRef]

26. Garfias, J.; Llanos, H.; Martel, R.; Salas-Garcia, J.; Bibiano-Cruz, L. Assessment of vulnerability and control measures to protect the Salbarua ecosystem from hypothetical spill sites. *Environ. Sci. Pollut. Res.* **2018**, *25*, 26228–26245. [CrossRef]

27. Barry, F.; Ophori, D.; Hoffman, J.; Canace, R. Groundwater flow and capture zone analysis of the Central Passaic River Basin, New Jersey. *Environ. Geol.* **2009**, *56*, 1593–1603. [CrossRef]

28. Shamsuddin, M.K.N.; Suratman, S.; Zakaria, M.P.; Aris, A.Z.; Sulaiman, W.N.A. Particle tracking analysis of river-aquifer interaction via bank infiltration techniques. *Environ. Earth Sci.* **2014**, *72*, 3129–3142. [CrossRef]

29. Pollock, D.W. *User Guide for MODPATH Version 7—A Particle-Tracking Model for MODFLOW: U.S. Geological Survey Open-File Report 2016-1086*; U.S. Geological Survey: Reston, VA, USA, 2016; p. 35. [CrossRef]

30. Yang, W.; Mao, W.; Yang, Y.; Zhu, Y.; Yang, J. Optimizing Conjunctive Use of Groundwater and Cannel Water in Hetao Irrigation District Aided by MODFLOW. *J. Irrig. Drain.* **2021**, *40*, 93–101. [CrossRef]

31. GUO, Y.; TIAN, X.; Zhang, L. Characteristics of Carbon Tetrachloride Pollution in Groundwater in a Water Source. *South North Water Divers. Water Sci. Technol.* **2011**, *9*, 109–113. [CrossRef]

32. Islam, M.R.; Jewett, D.; Williams, J.R.; Hantush, M. Calibration of groundwater flow and contaminant transport modeling for Ogallala, Nebraska. In Proceedings of the International Water Resources Engineering Conference on Water Resources Development and Protection, Memphis, TN, USA, 3–7 August 1998; pp. 105–110.